FOLIA HISTOCHEMICA ET CYTOBIOLOGICA
Vol. 61, No. 1, 2023
pp. 34–46

ORIGINAL ARTICLE

VIA MEDICA

Overexpressing six-transmembrane protein of prostate 2 (STAMP2) alleviates sepsis-induced acute lung injury probably by hindering M1 macrophage polarization *via* the NF-κB pathway

Lili Ji[1, 2], Xiaojing Shi[2], Gaopin Wang[3], Huiping Wu[4], Zhansheng Hu[1, 4]

[1]Medical College of Soochow University, Suzhou, Jiangsu, People's Republic of China

[2]Department of Emergency Medicine, The First Affiliated Hospital of Jinzhou Medical University, Jinzhou, Liaoning, People's Republic of China

[3]Department of Cardiology, The First Affiliated Hospital of Jinzhou Medical University, Jinzhou, Liaoning, People's Republic of China

[4]Department of Intensive Care Unit, The First Affiliated Hospital of Jinzhou Medical University, Jinzhou, Liaoning, People's Republic of China

Graphical abstract

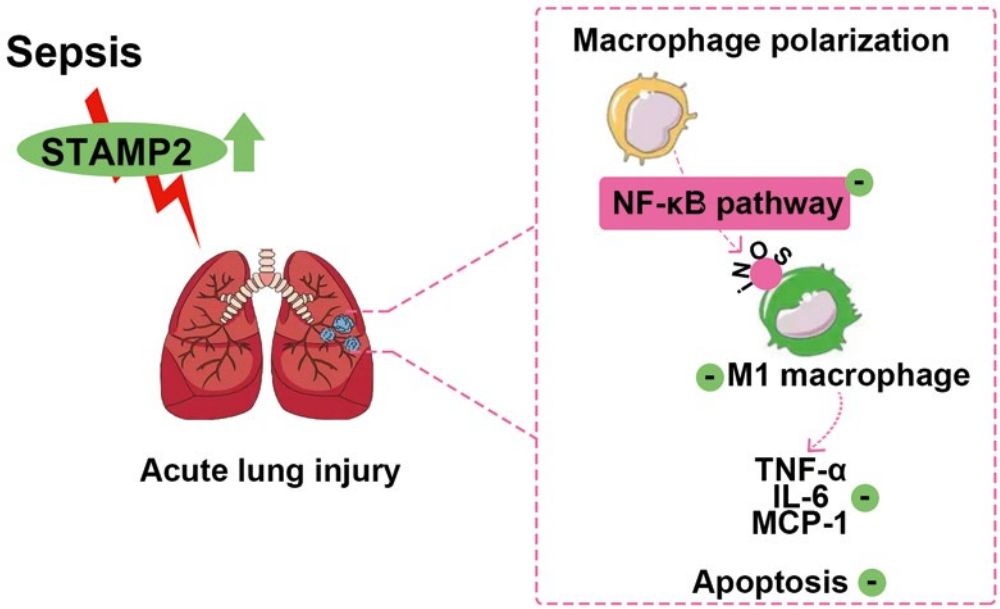

Correspondence address:
Dr. Zhansheng Hu
Medical College of Soochow University, No. 1, Shizi Street, Suzhou, Jiangsu, People's Republic of China

Department of Intensive Care Unit, The First Affiliated Hospital of Jinzhou Medical University, No. 2, Section 5, Renmin Street, Jinzhou, Liaoning, People's Republic of China
e-mail: icuhzs1969@163.com

Folia Histochem Cytobiol. 2023
10.5603/FHC.a2022.0032
ISSN 0239-8508, e-ISSN 1897-5631

Abstract

Introduction. Acute lung injury (ALI) is a major cause of death in sepsis patients. The Six-transmembrane protein of prostate 2 (STAMP2) is a key regulator of inflammation, while its role in septic ALI remains unclear.

Material and methods. Male C57BL/6 mice were subjected to cecal ligation puncture (CLP) to induce experimental sepsis whereas lipopolysaccharide (LPS)-stimulated RAW 264.7 cells were used as the models of septic ALI *in vivo* and *in vitro*, respectively. Overexpression of STAMP2 in mouse lungs and RAW264.7 cells was performed with an adenoviral vector. We measured histological lung injury, lung wet/dry weight (W/D) ratio, and pulmonary myeloperoxidase (MPO) activity to assess lung injury extent. Cell counts in bronchoalveolar lavage fluid (BALF) were measured using Giemsa staining. The concentration of inflammatory factors was detected by enzyme-linked immunosorbent assay. The polarization of macrophages was evaluated by inducible nitric oxide synthase (iNOS) and F4/80 staining. The activation of cell apoptosis and NF-κB pathway was evaluated using Western blot, TUNEL staining, immunofluorescence, and immunohistochemistry.

Results. Overexpression of STAMP2 alleviated CLP-induced lung injury of mice with decreased W/D ratio of the lung, and MPO activity in lung tissue. STAMP2 overexpression reduced the lung infiltration of inflammatory cells, and the levels of TNF-a, IL-6, and macrophage chemoattractant protein-1 (MCP-1) in BALF. Overexpressed STAMP2 inhibited macrophage M1 polarization in lung tissues as indicated by F4/80 and iNOS stainings in lung tissue. STAMP2 overexpression inhibited RAW 264.7 cell apoptosis by increasing Bcl-2 and decreasing Bax and cleaved-caspase 3 expression. Besides, STAMP2 overexpression suppressed nuclear factor κB (NF-κB) p65 pathway activation, as evidenced by reduced phosphorylation of IκBα, and phosphorylation and translocation of NF-κB p65. *In vitro* study further proved that STAMP2 overexpression suppressed the NF-κB pathway (IκBα/p65) in macrophages and decreased macrophage M1 polarization and M1-associated inflammatory factor production (TNF-a, IL-6, and MCP-1).

Conclusions. Our study for the first time demonstrated that STAMP2 might be able to reduce inflammation in sepsis-induced ALI by inhibiting macrophage M1 polarization through repressing NF-κB signaling activation. (*Folia Histochemica et Cytobiologica 2023, Vol. 61, No. 1, 34–46)*

Keywords: mouse; STAMP2; septic acute lung injury; inflammation; macrophage; NF-κB pathway

Introduction

Sepsis is a severe disease/state characterized by a severe systemic inflammatory response with high morbidity and mortality [1, 2]. Sepsis-induced damage, shock, and multi-organ dysfunction remain the leading causes of death in patients with sepsis [3]. As one of the main complications of sepsis, acute lung injury (ALI) is a destructive disease characterized by respiratory failure, alveolar-capillary membrane barrier disruption, pulmonary edema, and immune/inflammatory response [4]. Clinically, ALI is defined as acute respiratory distress syndrome (ARDS) and is recognized as one of the most direct causes of death in septic patients [5]. In lungs, macrophages, important innate immunity cells, present two major populations that are differently localized: (i) alveolar macrophages (AM) which populate alveoli and airways, and (ii) interstitial macrophages (IM) which reside in lung parenchyma [6, 7]. Activated macrophages are thought to be the pathological hallmark of the immune/inflammatory response in ALI [8, 9]. Despite numerous studies attempting to explore the mechanisms of ALI, the pathogenesis of the disease is not fully understood. Meanwhile, most clinical treatments are designed to prevent the symptoms of sepsis-induced ALI, which cannot effectively reduce mortality [10].

Nuclear factor κB (NF-κB) represents a eukaryotic transcription factors family that is involved in many aspects of inflammation and immunity. The NF-κB family contains five members: p65, RelB, c-Rel, p50, and p52 [11]. They can form multiple homodimers or heterodimers to further regulate inflammatory response by binding to specific target genes. The p65/p50 dimers are the main protein complexes that regulate the transcription of responsive genes [12]. The p65/p50 dimers are present as inactive complexes in the cytoplasm by binding to specific NF-κB inhibitor α (IκBα) [13]. In response to multiple cell stimuli, IκBα undergoes dissociation and phosphorylation. The active p65/p50 NF-κB dimers are translocated into the nucleus to activate NF-κB-dependent target genes including those that encode tumor necrosis factor-α (TNF-α), interleukin-6 (IL-6), and monocyte chemoattractant protein-1 (MCP-1) [14, 15]. Enhanced NF-κB activation is correlated with poor outcomes in septic ALI patients [16]. The expression of NF-κB was shown to be markedly induced in lung tissue in the septic ALI mouse model, and its activation contributed to the development of this condition [17]. Numerous studies suggested that inhibition of NF-κB activation

might offer a potential treatment approach for sepsis--induced ALI [18–20].

The Six-transmembrane protein of prostate 2 (STAMP2), also called six-transmembrane epithelial antigen of prostate 4 (STEAP4), belongs to the six-transmembrane protein family with iron reductase activities [21]. It is expressed strictly in several tissues including the lung, placenta heart, and prostate [22]. Several pieces of research have shown that STAMP2 was involved in the regulation of inflammation, oxidative stress, apoptosis, and the metabolism of fatty acid and glucose [23–26]. Meanwhile, STAMP2 plays a pro-oncogenic role in diverse cancers including prostate [27] and colon cancer [28]. It was reported that STAMP2 promoted anti-inflammatory activities in multiple tissues, most prominently in lung tissues [22]. STAMP2 deficiency showed a substantial pro-inflammatory response in mice with pulmonary arterial hypertension and increased release of inflammatory factors [29]. Recently, STAMP2 was reported to be highly expressed in the peripheral blood of septic patients [30], indicating the possible role of STAMP2 in sepsis-induced ALI. However, the potential role of STAMP2 in inhibiting septic ALI has not been explored yet. In our study, we proved that STAMP2 could attenuate sepsis-induced ALI by inhibiting the NF-κB signaling pathway in macrophages.

Materials and methods

Reagents and antibodies. pShuttle-CMV adenovirus vector was purchased from Fenghbio (Changsha, China). HEK--293A cell line was purchased from Procell (Wuhan, China). Western blotting and IP lysis buffer, Nuclear extraction kit, Bicinchoninic acid assay (BCA) kit, Enhanced chemiluminescent (ECL) kit, BeyoRT II M-MLV reverse transcriptase, and Triton X–100 were purchased from Beyotime Institute of Biotechnology (Shanghai, China). Dulbecco modified Eagle medium (DMEM) medium was purchased from Service biotechnology (Wuhan, China). TRIpure reagent was purchased from BioTeke Bio. (Beijing, China). Lipopolysaccharide (LPS), hematoxylin, and Reverse transcription quantitative real-time polymerase chain reaction (RT-qPCR) reagents were from Solarbio Science & Technology, Co., Ltd. (Beijing, China). 4', 6-diamidino-2-phenylindole (DAPI) was from Aladdin (Shanghai, China) 3, 3'-diaminobenzidine (DAB) was purchased from Maxinm Biotechnology (Fuzhou, China). Eosin was from Sangon Biotech (Shanghai, China). Mouse TNF-α, IL-6, and MCP-1 enzyme-linked immunosorbent assay (ELISA) kits were from LIANKE Biotech., Co., Ltd. (Hangzhou, China). Myeloperoxidase (MPO) activity kit and Giemsa staining solution were purchased from Jiancheng Bioengineering Institute (Nanjing, China). In situ cell death detection kit (Roche, Basel, Switzerland). The following antibodies were used: anti-iNOS, anti-F4/80, anti-phospho-IκBα, anti-IκBα, and anti-cleaved-caspase 3 were from Affbiotech (Changzhou, China); anti-phospho-p65 was from Novus Biologicals (Littleton, CO, USA); anti-p65 was from Cell Signaling Technology (Danvers, MA, USA); anti-STAMP2, anti-B cell lymphoma 2 (Bcl-2) and anti-Bcl2-Associated X (Bax) were from Proteintech Group, Inc. (Wuhan, China); anti-Histone H3 was from Abgent (San Diego, CA, USA); anti-β-actin was from Santa Cruz (Dallas, TX, USA); anti-mouse IgG-horseradish peroxidase (HRP) and anti-rabbit IgG-HRP were from Beyotime Institute of Biotechnology (Shanghai, China) and Thermo Scientific (Pittsburgh, PA, USA). Anti-rabbit IgG-Cy3 and Lipofectamine 3000 were from Invitrogen (Carlsbad, CA, USA).

Bioinformatics analysis. Our study downloaded three gene expression datasets (GSE2411, GSE60088, and GSE34901) from Gene Expression Omnibus (GEO) database (https://www.ncbi.nlm.nih.gov/geo/). The GEO2R (https://www.ncbi.nlm.nih.gov/geo/geo2r) web tool was utilized to analyze differential expressed genes (DEGs) with a threshold of log2 fold change (FC) > 2 and $P < 0.01$. The overlapping DEGs in three datasets were identified using Venn diagrams (https://bioinfogp.cnb.csic.es/tools/venny/index.html), and the overlapping DEGs were retained for additional analysis. Subsequently, Gene ontology (GO) analysis and Kyoto Encyclopedia of Genes and Genomes (KEGG) pathway analysis were performed on the obtained DEGs in DAVID Bioinformatics Resources Database (http://david.abcc.ncifcrf.gov/).

Animals. Animal procedures were approved by the Ethics Committee of Jinzhou Medical University. Eight-to-ten-week-old male C57BL/6 mice were purchased from Beijing Hua Fukang Biotechnology Co. Ltd. (Beijing, China). Mice were housed in controlled conditions under a 12:12 light-dark cycle and with unrestricted access to food and water. The temperature and humidity of the animal facility were kept at 22 ± 1° and 45–55%.

The designed sequences of STAMP2 were cloned into pShuttle-CMV adenovirus vector to create STAMP2 overexpression vector, with an empty vector as control. Adenoviral particles were generated by transfecting HEK-293A cells with all adenoviral vectors using Lipofectamine 3000 according to the manufacturer's instructions. After transfection, whole cell lysates from HEK-293A cells were harvested and then filtered. The virus stock was frozen in –80°C. The viral titer was determined using a plaque-forming assay with HEK-293A cells under 1.25% low melting point agarose overlay after 9–11 days of culture.

For STAMP2 overexpression, mice were tail vein-injected with adenovirus overexpressing STAMP2 or negative control adenovirus [2 × 108 plaque forming unit (pfu) per mouse] [31]. Three days after the adenovirus injection, the mice were subjected to cecal ligation and puncture (CLP) surgery. CLP was performed as described [32]. Under aseptic conditions, the cecum was exposed by the laparotomy. Roughly, the cecum was ligated with silk and perforated twice with the needle. In sham-operated control animals, the cecum was exposed but

Folia Histochem Cytobiol. 2023
10.5603/FHC.a2022.0032
ISSN 0239-8508, e-ISSN 1897-5631

neither ligated nor punctured. BALF and lung tissues were obtained 24 h after surgery. Lungs were weighed at separation (wet lung weight), and the lung tissues were dried at 80° in the oven to a constant weight (dry lung weight). Pulmonary edema was quantified by the wet-to-dry (W/D) ratio. Another batch of animals was raised to observe the survival rates of different groups for 10 days.

BALF collection and cell counting. BALF was collected by flushing the right lung with PBS after ligation of the left lung. The aliquots were pooled to obtain the total sample for one mouse. BALF was centrifuged and resuspended in 500 μL PBS. The total number of cells was measured using a hemacytometer. Differential counting of neutrophils and macrophages, and cell smears were stained with Giemsa dye and counted under the microscope.

Cell culture. RAW 264.7 cells were purchased from iCell Bioscience Inc. (Shanghai, China). Cells were grown in DMEM complete culture medium at 37° in a 5% CO_2 incubator. For adenoviruses infection, RAW 267.4 cells were infected with 10 multiplicity of infection (MOI) of adenoviruses in DMEM medium for 24 h, and then the medium was replaced with fresh medium for another 24 h cultivation. The stimulation of bacterial endotoxin LPS is frequently applied to mimic sepsis *in vivo* [33]. Cells were stimulated with 100 ng/mL LPS for up to 24 h [34].

Hematoxylin and eosin (H&E), immunofluorescence (IF), and immunohistochemistry (IHC) stainings. H&E, IHC, and IF procedures were performed as previously described [35]. The fresh lung tissue of mice was dissected, fixed in 4% paraformaldehyde, and embedded in paraffin. Paraffin-embedded lung samples were continuously sectioned into 5 μm-thick slides. The lung tissue slides were stained with hematoxylin (5 min) and eosin (3 min) to determine the extent of lung injury [36]. For IHC, primary antibodies against STAMP2, F4/80, and p-p65 were used. The slides were incubated respectively overnight at 4° with primary antibodies: anti-STAMP2 (1:100 dilution), anti-F4/80 (1:100 dilution), anti-p-p65 (1:100 dilution), followed by secondary antibody (anti-rabbit IgG-HRP, 1:500 dilution) incubation. DAB and hematoxylin were utilized for chromogen development and counterstaining, respectively. For IF staining, the procedure was similar to the IHC. The lung sections were incubated with iNOS (1:100 dilution) and p65 (1:100 dilution) antibodies overnight. After washing, lung sections were immersed into anti-rabbit IgG-Cy3 (1:200 dilution) for an hour and imaged with a microscope.

Western blot analysis. Extraction of whole protein from tissues or cells was prepared using Western blotting and IP lysis buffer, while extraction of nuclear protein or cytosolic protein was prepared using a nuclear extraction kit. Protein concentrations were determined using a BCA kit. Protein samples were then prepared with 5× loading buffer. Samples were separated by sodium dodecyl sulphate-polyacrylamide gel electrophoresis (SDS-PAGE) using 1× SDS running buffer and transferred to polyvinylidene difluoride (PVDF) membrane using 1× Tris-Glycine transfer buffer. The membranes were immunoblotted with primary antibodies and corresponding secondary antibodies. Blots were developed with ECL luminous fluid and imaged by a Gel imaging system. Band intensities were normalized to β-actin or histone H3 levels.

RNA extraction and RT-qPCR. Samples were flash-frozen in liquid nitrogen and stored at –80°C prior to total RNA extraction. RNA was extracted using TRIpure reagent, and its concentration was estimated by Nanodrop 2000. Reverse transcription was performed using BeyoRT II M-MLV reverse transcriptase. The cDNA was subjected to RT-qPCR using primers specific to STAMP2: 5′-CCCACTGGACCAAGGAT-3′ (forward); 5′-AGAAGACGCACAGCACA-3′ (reverse). Relative quantifications were calculated using $2^{-\Delta\Delta CT}$ method.

Cytokine and MPO analysis. The levels of TNF-α, IL-6, and MCP in the BALF or the conditioned medium of cultured RAW cells was evaluated using an ELISA kit according to the manufacturer's instructions. Lung tissue was homogenized in MPO buffer supplied from MPO kit at 4°C at a ratio of 1:19 (tissue weight to buffer volume). MPO levels in homogenized lung tissues were detected by the MPO activity kit.

TUNEL staining. The procedures were conducted as described previously [37]. Paraffin-embedded lung tissues were permeabilized using 0.1% Triton X–100. The apoptotic cell in each group was detected using terminal deoxynucleotidyl transferase (TdT) dUTP nick-end labeling) (TUNEL) staining. TUNEL-positive nuclei were visualized under a light microscope.

Statistical analysis. Data were analyzed using GraphPad Prism 8 software. Data were presented as means and error bars represented standard deviation. One-way ANOVA test was used to assess significance. Survival curves were analyzed using Kaplan-Meier curves. Analyses with resultant $P < 0.05$ were determined significant.

Results

Identification of differentially expressed genes (DEGs)

To identify the key gene, three gene expression profiles (GSE2411, GSE60088, and GSE34901) were downloaded from the GEO database. A total of 29 up-regulated genes were screened out based on $P < 0.01$ and $logFC > 2$ (Fig. 1A), and the differential gene expression was visualized using a heat map (Fig. 1B). To further reveal the feature of the differential genes, in the GO analysis, and KEGG analysis were performed through the DAVID website. As Fig. 1C shows, the main biological process of DEGs mainly participated in the immune system process and inflammatory response, the main cellular component was the extracellular region, and the major molecular function was cytokine activity. In KEGG analysis, enriched pathways and diseases were varied, involving Cytokine-cytokine receptor interaction, Viral protein interaction with cytokine and cytokine receptor, Legio-

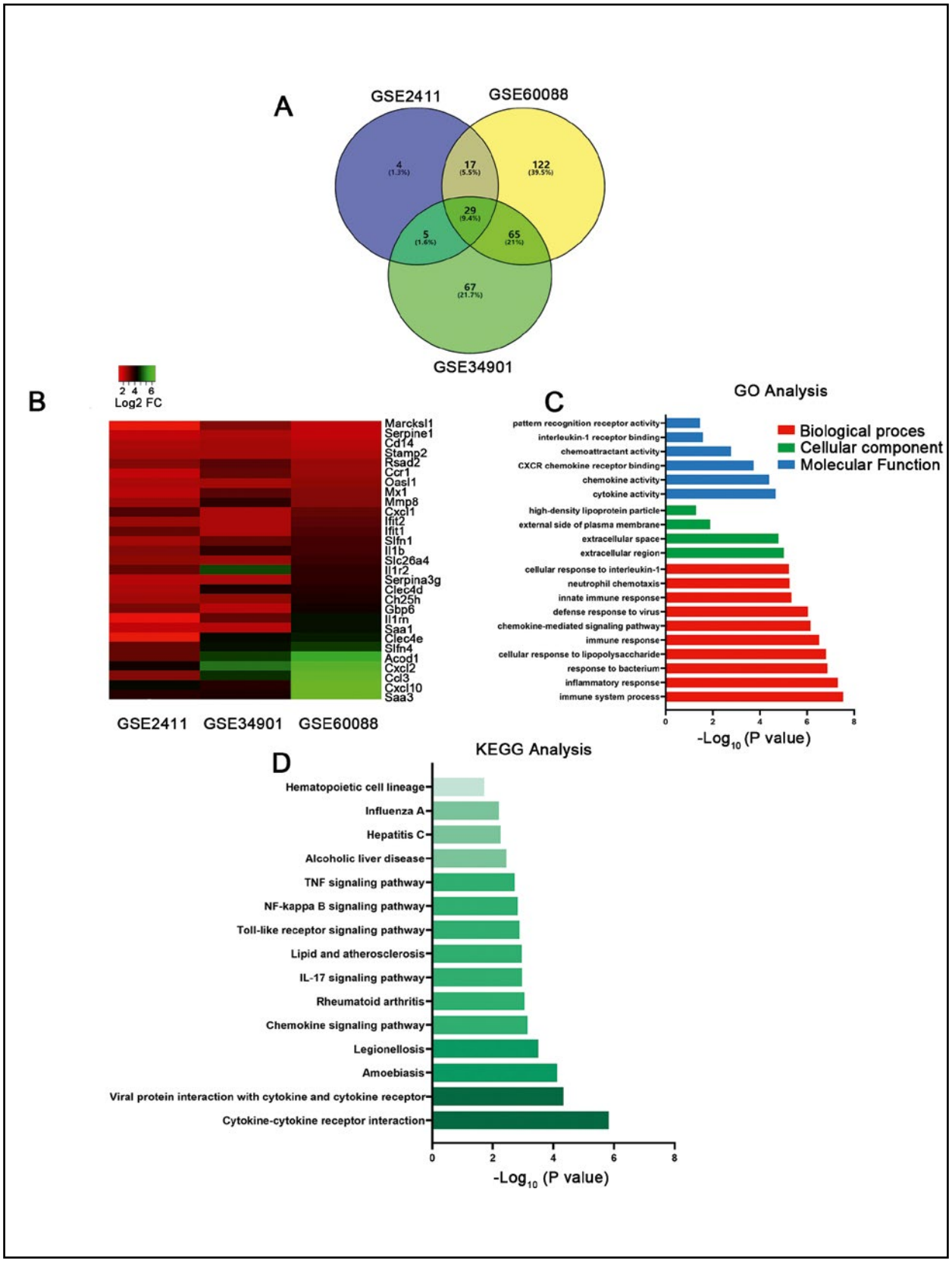

Figure 1. Identification of Differentially Expressed Genes (DEGs). **A.** Veen diagram of differentially expressed genes in GSE2411, GSE60088, and GSE34901 datasets. **B.** Heat map showing differential expression of 29 overlapping genes from 3 datasets. **C.** Gene ontology (GO) terms with the most significant P-value, including biological processes (shown top 10), cellular component, and molecular function. **D.** The top 15 Kyoto Encyclopedia of Genes and Genomes (KEGG) signaling pathways with the most significant P-value.

Folia Histochem Cytobiol. 2023
10.5603/FHC.a2022.0032
ISSN 0239-8508, e-ISSN 1897-5631

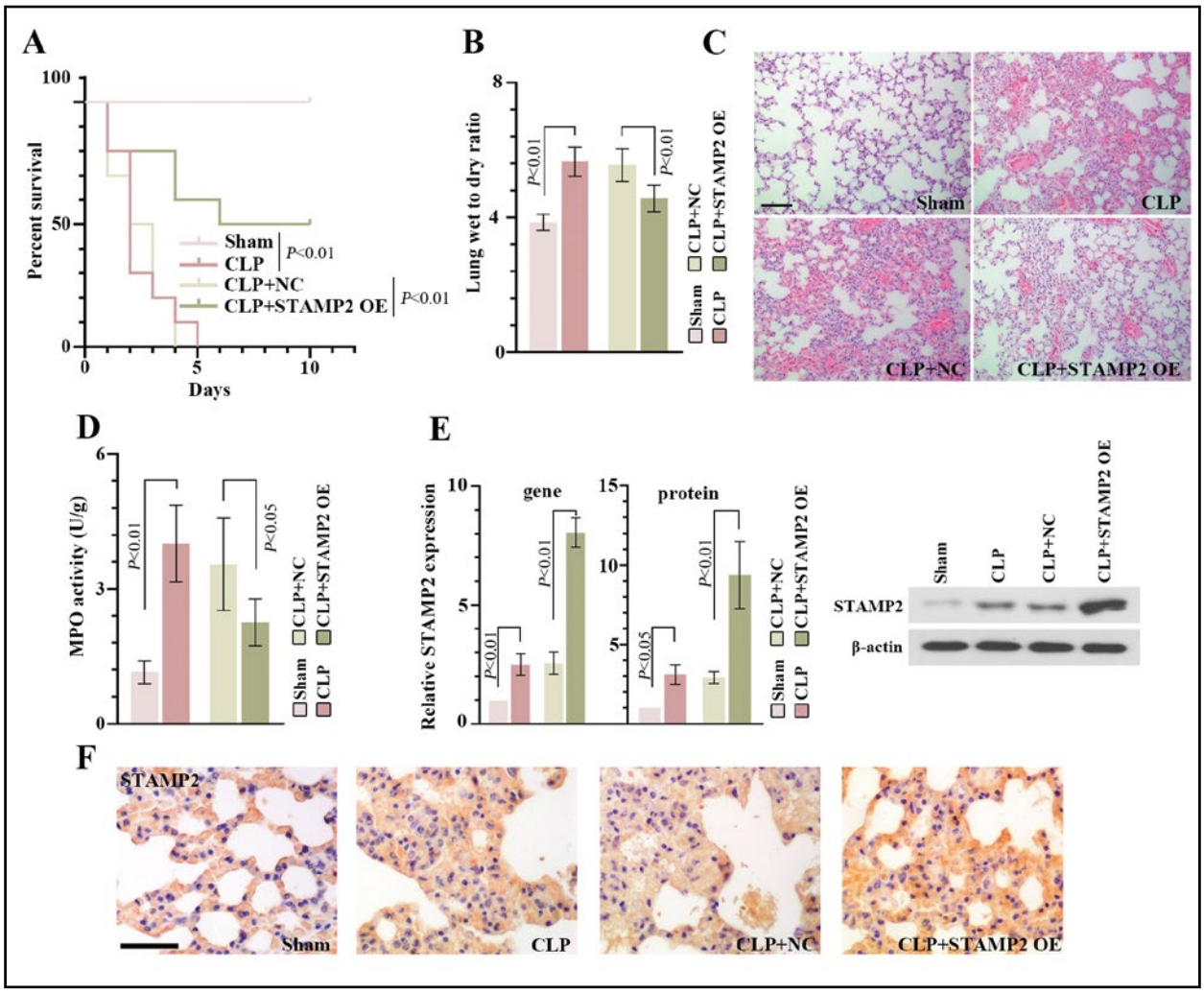

Figure 2. Overexpression of STAMP2 protects mice from sepsis-associated acute lung injury. **A.** Survival rate of mice in different treatment groups. **B.** Lung wet-to-dry ratios. **C.** The comparison of lung tissue H&E staining in mice of each treatment groups (200×, bar — 100 μm). **D.** MPO activity in lung homogenates. **E.** Left, gene and protein expression of STAMP2 in mouse lung tissues, β-actin served as endogenous control. Right, representative immunoblot of STAMP2. **F.** Immunohistochemistry assay of STAMP2 expression in lung tissue. (400×, bar — 50 μm). Data were expressed as the mean value ± SD. Abbreviations: CLP — cecall ligation and perforation; STAMP2, six-transmembrane protein of prostate 2; H&E — hematoxylin and eosin; MPO — myeloperoxidase; SD — standard deviation.

nellosis, Amoebiasis, Chemokine signaling pathway, Chemokine signaling pathway, NF-κB signaling pathway and so on (Fig. 1D). Among overlapping DEGs, multiple genes in sepsis has been reported such as Saa3, Acod1, CXCL family, and IL family. Through consulting literature, the STAMP2 was implicated in sepsis progression [30]. We, therefore, examined the possibility of STAMP2 in septic ALI.

Overexpression of STAMP2 protects mice from sepsis-associated acute lung injury

To determine the role of STAMP2 in septic ALI, we first evaluated whether STAMP2 overexpression could affect the mortality of CLP model mice. The decreased survival rate of septic mice (Fig. 2A), increased W/D ratio (Fig. 2B), and pathological changes in lung tissue (Fig. 2C) indicated the successful establishment of a mouse model of sepsis-induced ALI. Histopathologic analysis showed apparent infiltration of inflammatory cells and edema in lung tissues of mice induced by CLP (Fig. 2C). The overexpressed-STAMP2 obviously improved the survival of CLP-treated mice (Fig. 2A). Meanwhile, in septic lung tissues, an increase in mRNA and protein expression of STAMP2 was found (Fig. 2E). Besides, IHC staining results were consistent with the results of RT-qPCR and Western blot assays (Fig. 2F). The overexpression of STAMP2 decreased the W/D ratio of lung tissue (Fig. 2B) and improved the aberrant histopathological manifestations (Fig. 2C). In addition, CLP markedly increased lung MPO activity, while STAMP2 overexpression resulted in decreased MPO activity (Fig. 2D). These results in-

Folia Histochem Cytobiol. 2023
10.5603/FHC.a2022.0032
ISSN 0239-8508, e-ISSN 1897-5631

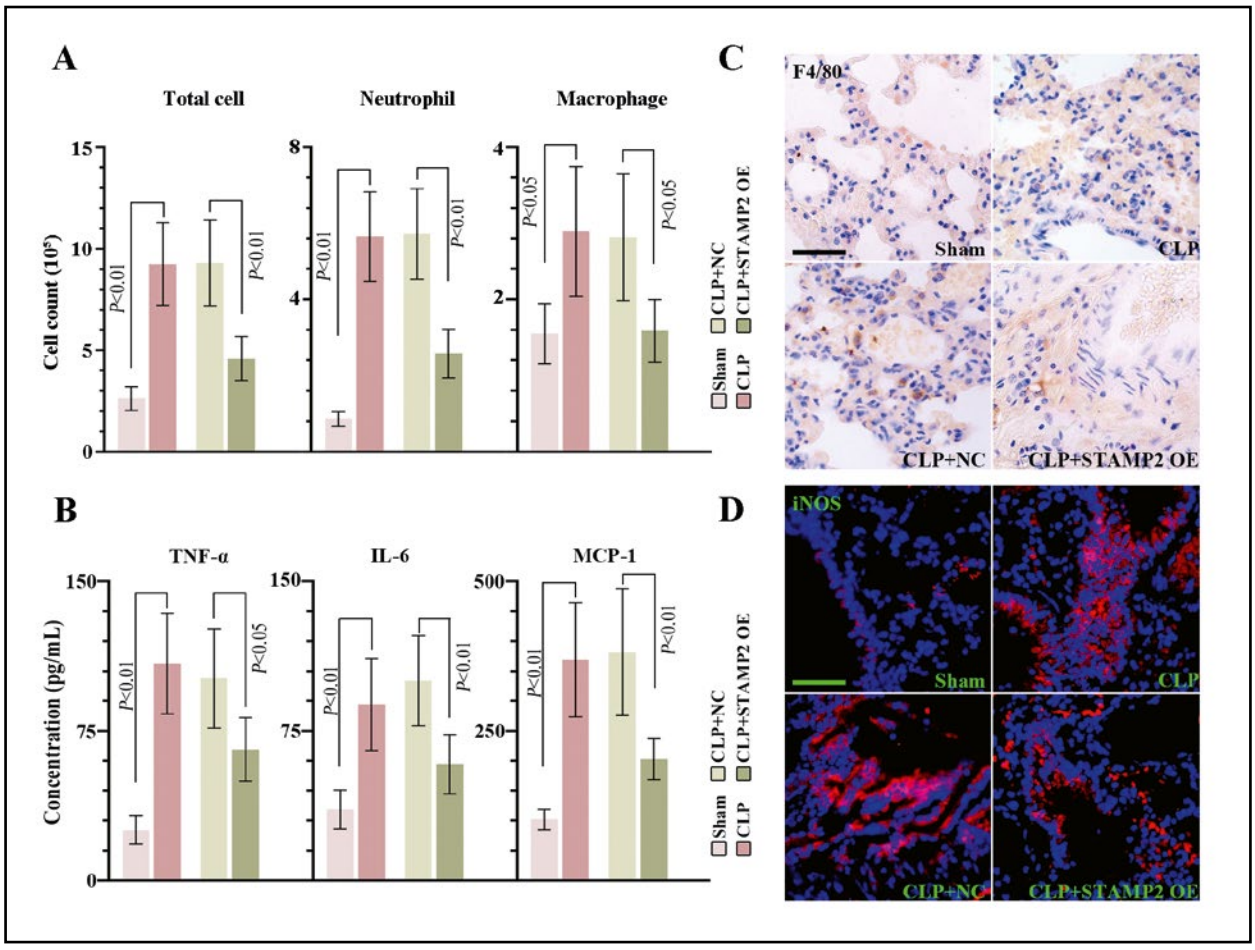

Figure 3. Overexpression of STAMP2 reduced CLP-induced macrophage activation and inflammatory response in mouse lung tissues. **A.** Total number of cells, neutrophils, and macrophages was counted in BALF by Giemsa staining. **B.** ELISA measurement of TNF-α, IL-6 and MCP-1 in BALF. **C.** Immunohistochemistry assay of F4/80 expression in lung tissues sections. **D.** Representative immunofluorescence iNOS staining of mouse lung tissues. Data were expressed as the mean value ± SD. Abbreviations: BALF — bronchoalveolar lavage fluid; iNOS — inducible nitric oxide synthase; ELISA — enzyme-linked immunosorbent assay; TNF-α — tumor necrosis factor α; IL-6 — interleukin-6; MCP-1 — monocyte chemoattractant protein-1.

dicated that STAMP2 might play a protective role in sepsis-induced ALI.

Overexpression of STAMP2 reduced CLP-induced macrophage activation and inflammatory response in mouse lung tissues

Compared with sham-operated mice, the CLP challenge significantly induced a higher amount of total cells, especially neutrophils and macrophages in BALF (Fig. 3A). Whereas, overexpressed-STAMP2 decreased the numbers of the cells (Fig. 3A). Regarding the inflammation markers, the levels of TNF-α, IL-6, and MCP-1 in BALF were significantly decreased by STAMP2 overexpression (Fig. 3B). In STAMP2 overexpression mice, we observed decreased number of pro-inflammatory macrophages and polarized macrophages as proved by decreased expression of macrophage marker F4/80 antigen (Fig. 3C) and iNOS (M1 macrophage polarization indicator) (Fig. 3D). These observations suggested that STAMP2 might inhibit inflammatory response by suppressing inflammatory factors' release and macrophage polarization.

Overexpression of STAMP2 mitigates CLP-induced cell apoptosis of lung tissue

A pronounced increase in cell apoptosis in lung tissue detected by the TUNEL staining was observed in CLP-treated mice, which was noticeably attenuated by STAPM2 overexpression (Fig. 4A). Consistently, CLP induced a clear increase in Bax expression and a decrease in Bcl-2 and cleaved-caspase 3 expression in lung tissues of mice with septic ALI, which was reversed by STAPM2 overexpression (Fig. 4B).

Folia Histochem Cytobiol. 2023
10.5603/FHC.a2022.0032
ISSN 0239-8508, e-ISSN 1897-5631

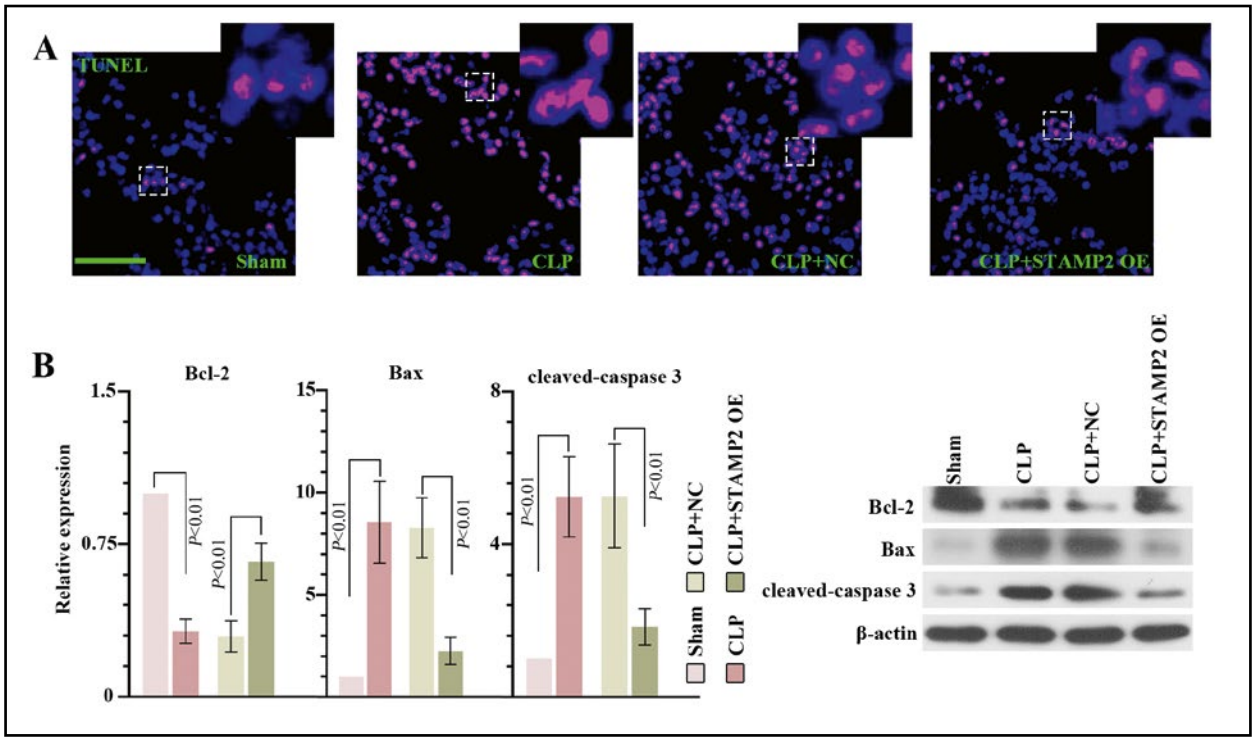

Figure 4. Overexpression of STAMP2 mitigates CLP-induced apoptosis of lung tissues. **A.** Cell apoptosis was visualized by the TUNEL staining. **B.** Left, the protein expression of Bax, Bcl-2 and cleaved-caspase 3 in mouse lung tissues. Right, representative immunoblot of Bax, Bcl-2 and cleaved-caspase 3. β-actin served as endogenous control. Data were expressed as the mean value ± SD. TUNEL, terminal deoxynucleotidyl transferase-mediated dUTP nick end labeling; Bax, Bcl2-Associated X; Bcl-2, B cell lymphoma/lewkmia-2.

Effects of STAMP2 on NF-κB pathway components in CLP-treated mice

Given the central role of NF-κB signaling in septic ALI [17], the effect of STAMP2 on NF-κB signaling was explored. Western blot and immunofluorescence methods were employed to analyze the activation of NF-κB signaling. Western blot results showed that CLP significantly increased the expression of p-IκBα (Fig. 5A), p-p65, and nuclear p65 (Fig. 5B) and decreased the expression of IκBα (Fig. 5A) in lung tissues of mice. On the contrary, overexpression of STAMP2 resulted in a marked increase in IκBα expression and a decrease in p-IκBα, p-p65, and nuclear p65 expression (Fig. 5A–C). Meanwhile, the expression of p-p65 in lung tissues detected by IHC staining revealed the inhibition effect of STAMP2 on p-p65 (Fig. 5D).

Effect of STAMP2 on NF-κB signaling in LPS-induced RAW267.4 cells

Lipopolysaccharide, LPS, a lipoglycan present in the cell membranes of Gram-negative bacteria, has been widely used to induce ALI both *in vivo* and to stimulate cells *in vitro*. The RAW 264.7 cells (a macrophage cell line) were incubated with LPS. STAMP2 was adenovirally overexpressed in cells to explore the role of STAMP2 in macrophages. Transfection efficiency was validated by RT-qPCR and Western blotting (Fig. 6A). Our results revealed that the supernatants from cultured STAMP2-overexpressing RAW264.7 cells stimulated with LPS contained lower levels of TNF-α, IL-6, and MCP-1 than that from control cells (Fig. 6B). The iNOS expression was also decreased upon STAMP2 overexpression in RAW264.7 macrophages (Fig. 6C). As shown in Fig. 6D–E, STAMP2 overexpression significantly inhibited the activation of NF-κB signaling in LPS-stimulated cells. STAMP2 overexpression inhibited the nuclear translocation of NF-κB p65 (Fig. 6D). Moreover, STAMP2 overexpression markedly decreased the phosphorylation of IκBα, p65, and nuclear p65 expression, and increased IκBα expression (Fig. 6E).

Discussion

Sepsis is a dysregulated host response to infection, resulting in life-threatening organ dysfunction [38]. The lung is the most vulnerable and important organ during the pathogenesis of sepsis. The mortality rate of ALI exceeds 40%, causing a huge economic and social

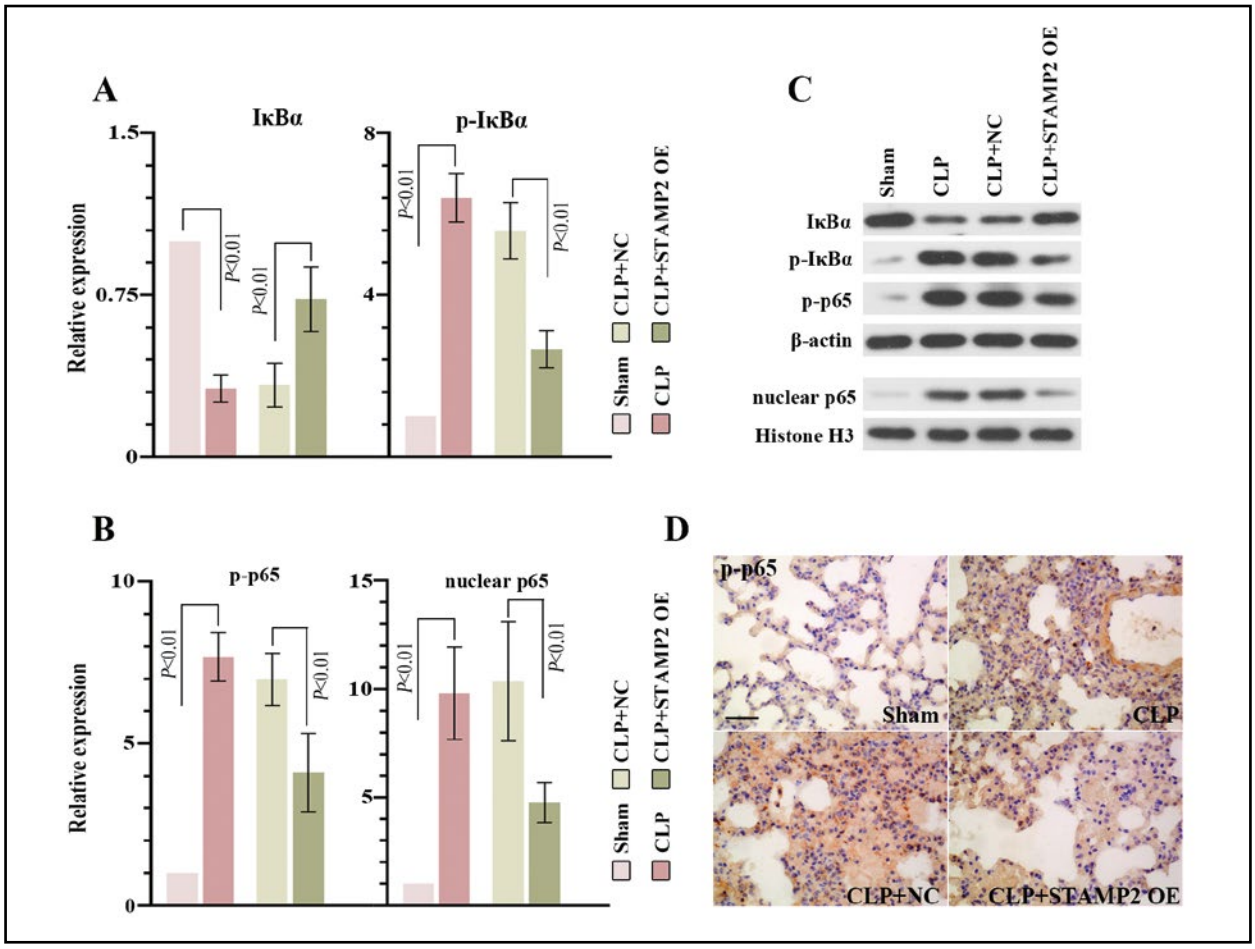

Figure 5. Effects of STAMP2 on NF-**κB** pathway components in CLP-treated mice. **A, B.** The quantification of IκBα (A), p-IκBα (A), p-p65 (B), and nuclear p65 (B) protein expression. **C.** Representative immunoblot of IκBα, p-IκBα, p-p65 and nuclear p65. **D.** Representative images of p-p65 immunohistochemistry staining of mouse lung tissues. β-actin and Histone H3 served as endogenous control. Data were expressed as the mean value ± SD.

burden [39]. In our study, the CLP-induced murine ALI model exhibited various typical sepsis characteristics, including reduced survival rate, histopathological, physiological, and biochemical indices, and increased serum cytokine levels, indicating the successful establishment of the sepsis-induced ALI model. [5, 40].

STAMP2 is reported to coordinate inflammatory responses with metabolic function and has been reported to be essential for metabolic homeostasis to coordinate pulmonary inflammation in mice [24]. In our study, higher expression of STAMP2 in the lung tissue of CLP-treated mice was observed. Meanwhile, STAMP2 overexpression decreased the survival rate and alleviated sepsis-induced ALI in mice. In BALF, lower leucocytes, macrophages, and neutrophils numbers and inflammatory cytokines' levels were also observed.

Leukocytes, including neutrophils and macrophages, usually found in BALF, have been reported to contribute to ALI [8]. As the most common pulmonary immune cells [41], macrophages play a critical role in septic ALI. The recruited and activated macrophages can release pro-inflammatory cytokines, and induce neutrophil infiltration, further aggravating inflammatory response, disrupting the endothelial barrier, and exacerbating lung injury [42, 43]. Our study is the first to report the anti-inflammatory effects of STAMP2 in septic ALI demonstrated by decreased MPO activity in mice overexpressing STAMP2. We suggest that increased STAMP2 levels in septic inflammatory states may be due to its compensatory anti-inflammatory effect.

Macrophages are essential for pulmonary homeostasis and immune responses to pathogens [44]. In the early stages of ALI development, macrophages can polarize into classically activated macrophages of the M1 type [45]. M1 macrophages release pro-inflammatory cytokines including TNF-α, IL-6, and MCP-

Folia Histochem Cytobiol. 2023
10.5603/FHC.a2022.0032
ISSN 0239-8508, e-ISSN 1897-5631

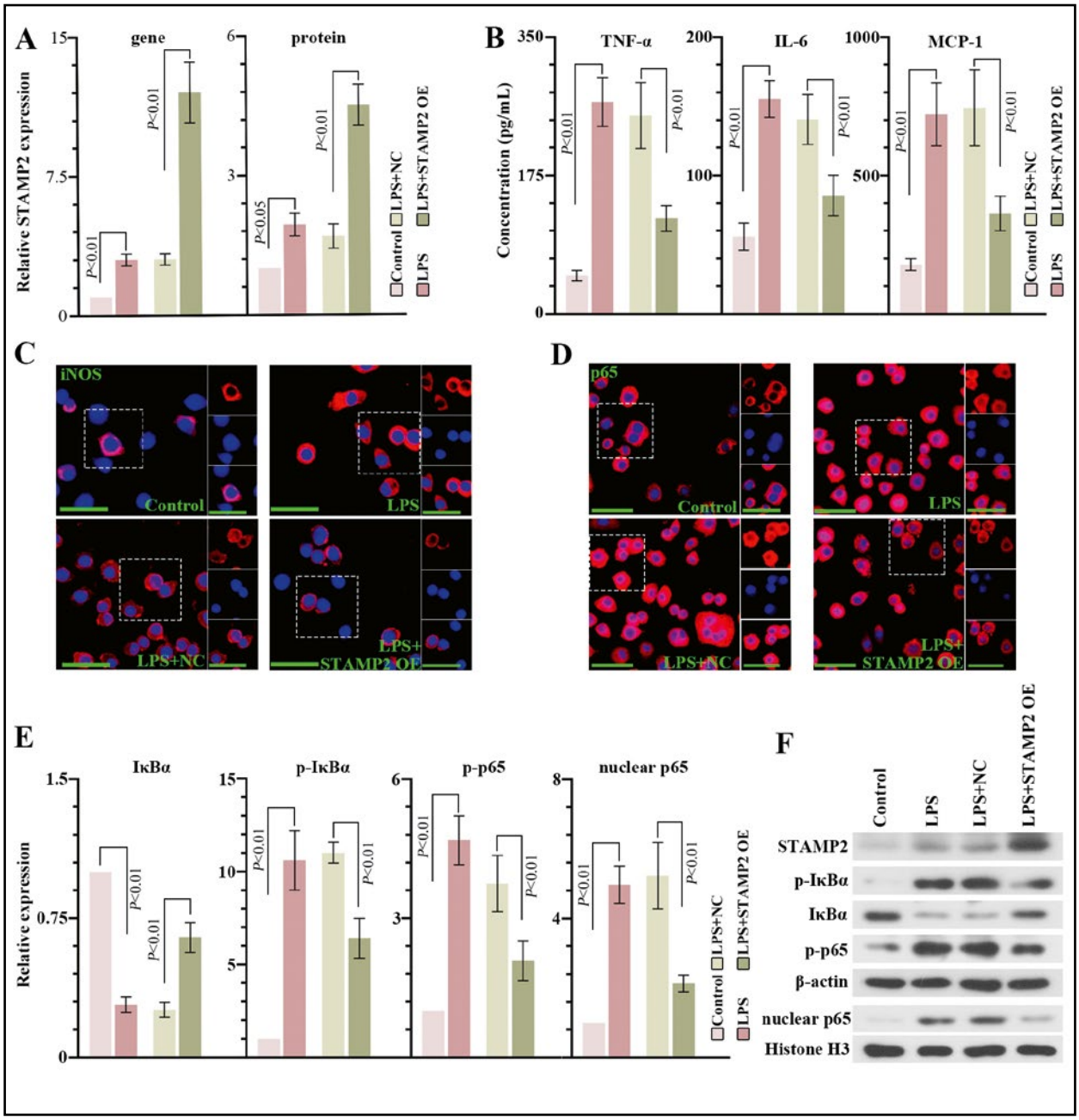

Figure 6. Effect of STAMP2 on NF-κB signaling in LPS-induced RAW267.4 cells. **A.** Gene and protein expression of STAMP2 in RAW264.7 cells with LPS stimulation. **B.** ELISA measurement of TNF-α, IL-6 and MCP-1 in cell supernatant. **C–D.** Representative images of iNOS (A) and p65 (B) immunofluorescence staining. **E.** Quantification of IκBα, p-IκBα, p-p65 and nuclear p65 protein expression. **F.** Representative immunoblot of IκBα, p-IκBα, p-p65 and nuclear p65. β-actin and Histone H3 served as endogenous control. Data were expressed as the mean value ± SD.

1 [46]. Regulation of macrophage polarization has been proposed as a therapeutic strategy for sepsis-induced ALI [45]. F4/80 and iNOS are the surface marker of macrophages and M1-type macrophages, respectively. STAMP2 overexpression in our study decreased infiltration of F4/80-positive macrophages and induced iNOS-positive M1 macrophage polarization. Moreover, decreased levels of TNF-α, IL-6, and MCP-1 were observed in STAMP2 overexpression mice. In a mouse model of rheumatoid arthritis, STAMP2 was co-located with macrophage marker CD68 [47]. Han *et al.* reported that STAMP2 overexpression inhibited macrophage infiltration, M1 macrophage polarization, and pro-inflammatory factors' release in mouse epididymal and brown adipose tissues, improving insulin resistance [48]. Besides, STAMP2 knockdown could enhance the infiltration of macrophages in lung tissue and increase inflammatory output from

macrophages, worsening pulmonary vascular remodeling and hypertension in mice [29]. Therefore, in our septic ALI model, STAMP2 might reduce inflammation by inhibiting macrophage polarization.

Excessive and persistent inflammation is the primary hallmark of septic ALI. However, clinical findings suggested that anti-inflammatory drugs alone could not significantly improve ALI [49]. It was reported that, in sepsis or ALI, the inflammatory cascade induced apoptosis of alveolar cells, which impaired the barrier function of the lungs [50], and apoptosis can in turn amplify the inflammatory response [51]. Moon *et al.* [52] observed exacerbated hepatocyte apoptosis in sepsis-induced ALI, and the regulation of apoptosis could play a protective role in ALI. The involvement of STAMP2 in cell apoptosis has been reported in prostate cancer [27], which is similar to our results. In our study, we found that STAMP2 overexpression inhibited cell apoptosis in lung tissues of ALI mice by decreasing Bax and cleaved-caspase 3 expression and increasing Bcl-2 expression. Bcl-2 family proteins, including pro-apoptotic Bax and anti-apoptotic Bcl-2 protein are key regulators of apoptosis, which mediated the activation of caspase 3 (the final apoptotic executor) [53]. STAMP2 overexpression has been reported to inhibit cell apoptosis by decreasing cleaved caspase-3 expression in diabetic mice [54].

NF-κB signaling pathway has been considered to be critical in septic ALI. A number of studies indicated that the blockade of the NF-κB pathway is an important modality in the treatment of sepsis-induced ALI [55, 56]. NF-κB activation induces the release of pro-inflammatory mediators and the expression of apoptosis-related proteins, which is closely related to the pathogenesis of ALI [57]. To date, STAMP2 was reported to be involved in the regulation of inflammatory pathways not only in lung cells [29] but also in macrophages [58]. Our data provided novel evidence for the inhibitory role of STAMP2 on the NF-κB signal pathway in septic ALI mice and LPS-stimulated RAW264.7 cells. Moreover, STAMP2 overexpression also inhibited the polarization of RAW264.7 cells and release of inflammatory factors. NF-κB signaling is thought to be a key factor for macrophage M1 polarization [59]. The inhibition of NF-κB pathway could inhibit M1 macrophage polarization and then decrease the release of M1 macrophage-associated pro-inflammatory cytokines [60]. The regulatory role of STAMP2 on NF-κB signaling has been reported in a murine model of ischemia and reperfusion [61]. However, the specific mechanism of STAMP2 action on NF-κB signaling in macrophages remains unclear. Taken together, our results suggested that STAMP2 might reduce inflammation by inhibiting M1 macrophage polarization through the NF-κB signaling pathway, thereby alleviating sepsis-induced ALI.

In conclusion, to the best of our knowledge, this is the first mechanical study of STAMP2 effects in sepsis-induced ALI. Our study offers insights into the molecular mechanisms of STAMP2 in the pathogenesis and treatment of sepsis-induced ALI.

Conflict of interest

The authors declare no conflict of interest.

Authors contribution

LILI JI: Conceptualization, Design, Methodology, Visualization, Writing — Original Draft. XIAOJING SHI: Methodology, Validation, Design. GAOPIN WANG: Validation, Visualization. HUIPING WU: Visualization; ZHANSHENG HU: Conceptualization, Supervision, Writing — Review & Editing.

References

1. Ferrer R, Artigas A, Suarez D, et al. Edusepsis Study Group. Effectiveness of treatments for severe sepsis: a prospective, multicenter, observational study. Am J Respir Crit Care Med. 2009; 180(9): 861–866, doi: 10.1164/rccm.200812-1912OC, indexed in Pubmed: 19696442.
2. Angus DC, van der Poll T. Severe sepsis and septic shock. N Engl J Med. 2013; 369(9): 840–851, doi: 10.1056/NEJMra1208623, indexed in Pubmed: 23984731.
3. Singer M, Deutschman CS, Seymour CW, et al. The third international consensus definitions for sepsis and septic shock (sepsis-3). JAMA. 2016; 315(8): 801–810, doi: 10.1001/jama.2016.0287, indexed in Pubmed: 26903338.
4. Thompson BT, Chambers RC, Liu KD, et al. Acute respiratory distress syndrome. N Engl J Med. 2017; 377(6): 562–572, doi: 10.1056/NEJMra1608077, indexed in Pubmed: 28792873.
5. Song Yi, Wu Q, Jiang H, et al. The effect of shionone on sepsis-induced acute lung injury by the ECM1/STAT5/NF-κB pathway. Front Pharmacol. 2021; 12: 764247, doi: 10.3389/fphar.2021.764247, indexed in Pubmed: 35153740.
6. Butt Y, Kurdowska A, Allen TC. Acute lung injury: a clinical and molecular review. Arch Pathol Lab Med. 2016; 140(4): 345–350, doi: 10.5858/arpa.2015-0519-RA, indexed in Pubmed: 27028393.
7. Hussell T, Bell TJ. Alveolar macrophages: plasticity in a tissue-specific context. Nat Rev Immunol. 2014; 14(2): 81–93, doi: 10.1038/nri3600, indexed in Pubmed: 24445666.
8. Fowler AA, Truwit JD, Hite RD, et al. Effect of Vitamin C Infusion on Organ Failure and Biomarkers of Inflammation and Vascular Injury in Patients With Sepsis and Severe Acute Respiratory Failure: The CITRIS-ALI Randomized Clinical Trial. JAMA. 2019; 322(13): 1261–1270, doi: 10.1001/jama.2019.11825, indexed in Pubmed: 31573637.
9. Zhang ZT, Zhang DY, Xie Ke, et al. Luteolin activates Tregs to promote IL-10 expression and alleviating caspase-11-dependent pyroptosis in sepsis-induced lung injury. Int Immunopharmacol. 2021; 99: 107914, doi: 10.1016/j.intimp.2021.107914, indexed in Pubmed: 34246059.
10. Song J, Chen D, Pan Y, et al. Discovery of a novel MyD88 inhibitor M20 and its protection against sepsis-mediated acute

lung injury. Front Pharmacol. 2021; 12: 775117, doi: 10.3389/fphar.2021.775117, indexed in Pubmed: 34912226.
11. May MJ, Ghosh S. Rel/NF-kappa B and I kappa B proteins: an overview. Semin Cancer Biol. 1997; 8(2): 63–73, doi: 10.1006/scbi.1997.0057, indexed in Pubmed: 9299584.
12. Beinke S, Ley SC. Functions of NF-kappaB1 and NF-kappaB2 in immune cell biology. Biochem J. 2004; 382(Pt 2): 393–409, doi: 10.1042/BJ20040544, indexed in Pubmed: 15214841.
13. Ramakrishnan P, Wang W, Wallach D. Receptor-specific signaling for both the alternative and the canonical NF-kappaB activation pathways by NF-kappaB-inducing kinase. Immunity. 2004; 21(4): 477–489, doi: 10.1016/j.immuni.2004.08.009, indexed in Pubmed: 15485626.
14. Baldwin Jr AS. The NF-kappa B and I kappa B proteins: new discoveries and insights. Annu Rev Immunol. 1996; 14: 649–683, doi: 10.1146/annurev.immunol.14.1.649, indexed in Pubmed: 8717528.
15. Ghosh S, May MJ, Kopp EB. NF-kappa B and Rel proteins: evolutionarily conserved mediators of immune responses. Annu Rev Immunol. 1998; 16: 225–260, doi: 10.1146/annurev.immunol.16.1.225, indexed in Pubmed: 9597130.
16. Yang KY, Arcaroli JJ, Abraham E. Early alterations in neutrophil activation are associated with outcome in acute lung injury. Am J Respir Crit Care Med. 2003; 167(11): 1567–1574, doi: 10.1164/rccm.200207-664OC, indexed in Pubmed: 12626346.
17. Li J, Ma J, Li M, et al. GYY4137 alleviates sepsis-induced acute lung injury in mice by inhibiting the PDGFRβ/Akt/NF-κB/NLRP3 pathway. Life Sci. 2021; 271: 119192, doi: 10.1016/j.lfs.2021.119192, indexed in Pubmed: 33577850.
18. Lee EH, Shin MiH, Gi M, et al. Inhibition of Pendrin by a small molecule reduces Lipopolysaccharide-induced acute Lung Injury. Theranostics. 2020; 10(22): 9913–9922, doi: 10.7150/thno.46417, indexed in Pubmed: 32929324.
19. Ren Q, Guo F, Tao S, et al. Flavonoid fisetin alleviates kidney inflammation and apoptosis via inhibiting Src-mediated NF-κB p65 and MAPK signaling pathways in septic AKI mice. Biomed Pharmacother. 2020; 122: 109772, doi: 10.1016/j.biopha.2019.109772, indexed in Pubmed: 31918290.
20. Wang YM, Ji R, Chen EZ, et al. Paclitaxel alleviated sepsis-induced acute lung injury by activating MUC1 and suppressing TLR-4/NF-κB pathway. Drug Des Devel Ther. 2019; 13: 3391–3404, doi: 10.2147/DDDT.S222296, indexed in Pubmed: 31576113.
21. Sikkeland J, Sheng X, Jin Y, et al. STAMPing at the crossroads of normal physiology and disease states. Mol Cell Endocrinol. 2016; 425: 26–36, doi: 10.1016/j.mce.2016.02.013, indexed in Pubmed: 26911931.
22. Yoo SK, Cheong J, Kim HY. STAMPing into mitochondria. Int J Biol Sci. 2014; 10(3): 321–326, doi: 10.7150/ijbs.8456, indexed in Pubmed: 24643198.
23. Grunewald TGP, Bach H, Cossarizza A, et al. The STEAP protein family: versatile oxidoreductases and targets for cancer immunotherapy with overlapping and distinct cellular functions. Biol Cell. 2012; 104(11): 641–657, doi: 10.1111/boc.201200027, indexed in Pubmed: 22804687.
24. Wellen KE, Fucho R, Gregor MF, et al. Coordinated regulation of nutrient and inflammatory responses by STAMP2 is essential for metabolic homeostasis. Cell. 2007; 129(3): 537–548, doi: 10.1016/j.cell.2007.02.049, indexed in Pubmed: 17482547.
25. Waki H, Tontonoz P. STAMPing out inflammation. Cell. 2007; 129(3): 451–452, doi: 10.1016/j.cell.2007.04.022, indexed in Pubmed: 17482536.
26. Gomes IM, Maia CJ, Santos CR. STEAP proteins: from structure to applications in cancer therapy. Mol Cancer Res. 2012; 10(5): 573–587, doi: 10.1158/1541-7786.MCR-11-0281, indexed in Pubmed: 22522456.
27. Jin Y, Wang L, Qu Su, et al. STAMP2 increases oxidative stress and is critical for prostate cancer. EMBO Mol Med. 2015; 7(3): 315–331, doi: 10.15252/emmm.201404181, indexed in Pubmed: 25680860.
28. Liao Y, Zhao J, Bulek K, et al. Inflammation mobilizes copper metabolism to promote colon tumorigenesis via an IL-17-STEAP4-XIAP axis. Nat Commun. 2020; 11(1): 900, doi: 10.1038/s41467-020-14698-y, indexed in Pubmed: 32060280.
29. Batool M, Berghausen EM, Zierden M, et al. The six-transmembrane protein Stamp2 ameliorates pulmonary vascular remodeling and pulmonary hypertension in mice. Basic Res Cardiol. 2020; 115(6): 68, doi: 10.1007/s00395-020-00826-8, indexed in Pubmed: 33188479.
30. Jiang H, Dong Y, Yan D, et al. The expression of STEAP4 in peripheral blood predicts the outcome of septic patients. Ann Transl Med. 2021; 9(20): 1519, doi: 10.21037/atm-21-2794, indexed in Pubmed: 34790725.
31. Yano K, Liaw PC, Mullington JM, et al. Vascular endothelial growth factor is an important determinant of sepsis morbidity and mortality. J Exp Med. 2006; 203(6): 1447–1458, doi: 10.1084/jem.20060375, indexed in Pubmed: 16702604.
32. Cloonan SM, Glass K, Laucho-Contreras ME, et al. Mitochondrial iron chelation ameliorates cigarette smoke-induced bronchitis and emphysema in mice. Nat Med. 2016; 22(2): 163–174, doi: 10.1038/nm.4021, indexed in Pubmed: 26752519.
33. Matute-Bello G, Frevert CW, Martin TR. Animal models of acute lung injury. Am J Physiol Lung Cell Mol Physiol. 2008; 295(3): L379–L399, doi: 10.1152/ajplung.00010.2008, indexed in Pubmed: 18621912.
34. Iliev DB, Goetz GW, Mackenzie S, et al. Pathogen-associated gene expression profiles in rainbow trout macrophages. Comp Biochem Physiol Part D Genomics Proteomics. 2006; 1(4): 416–422, doi: 10.1016/j.cbd.2006.10.003, indexed in Pubmed: 20483273.
35. Meng F, Liu X, Lin C, et al. SMYD2 suppresses APC2 expression to activate the Wnt/β-catenin pathway and promotes epithelial-mesenchymal transition in colorectal cancer. Am J Cancer Res. 2020; 10(3): 997–1011, indexed in Pubmed: 32266106.
36. Hirano Y, Aziz M, Yang WL, et al. Neutralization of osteopontin attenuates neutrophil migration in sepsis-induced acute lung injury. Crit Care. 2015; 19(1): 53, doi: 10.1186/s13054-015-0782-3, indexed in Pubmed: 25887405.
37. Carracedo A, Lorente M, Egia A, et al. The stress-regulated protein p8 mediates cannabinoid-induced apoptosis of tumor cells. Cancer Cell. 2006; 9(4): 301–312, doi: 10.1016/j.ccr.2006.03.005, indexed in Pubmed: 16616335.
38. Chen XH, Yin YJ, Zhang JX. Sepsis and immune response. World J Emerg Med. 2011; 2(2): 88–92, doi: 10.5847/wjem.j.1920-8642.2011.02.002, indexed in Pubmed: 25214990.
39. Fein AM, Calalang-Colucci MG. Acute lung injury and acute respiratory distress syndrome in sepsis and septic shock. Crit Care Clin. 2000; 16(2): 289–317, doi: 10.1016/s0749-0704(05)70111-1, indexed in Pubmed: 10768083.
40. Gao M, Yu T, Liu D, et al. Sepsis plasma-derived exosomal miR-1-3p induces endothelial cell dysfunction by targeting SERP1. Clin Sci (Lond). 2021; 135(2): 347–365, doi: 10.1042/CS20200573, indexed in Pubmed: 33416075.
41. Kopf M, Schneider C, Nobs SP. The development and function of lung-resident macrophages and dendritic cells. Nat Immunol. 2015; 16(1): 36–44, doi: 10.1038/ni.3052, indexed in Pubmed: 25521683.
42. Wang Z, Rui T, Yang M, et al. Alveolar macrophages from septic mice promote polymorphonuclear leukocyte transendothelial migration via an endothelial cell Src kinase/NADPH oxidase

pathway. J Immunol. 2008; 181(12): 8735–8744, doi: 10.4049/jimmunol.181.12.8735, indexed in Pubmed: 19050294.
43. Park I, Kim M, Choe K, et al. Neutrophils disturb pulmonary microcirculation in sepsis-induced acute lung injury. Eur Respir J. 2019; 53(3): 1800786, doi: 10.1183/13993003.00786-2018, indexed in Pubmed: 30635296.
44. He W, Chen CJ, Mullarkey CE, et al. Alveolar macrophages are critical for broadly-reactive antibody-mediated protection against influenza A virus in mice. Nat Commun. 2017; 8(1): 846, doi: 10.1038/s41467-017-00928-3, indexed in Pubmed: 29018261.
45. Liu M, Chen Y, Wang S, et al. α-ketoglutarate modulates macrophage polarization through regulation of PPARγ transcription and mTORC1/p70S6K pathway to ameliorate ALI/ARDS. Shock. 2020; 53(1): 103–113, doi: 10.1097/SHK.0000000000001333, indexed in Pubmed: 31841452.
46. Murray PJ. Macrophage Polarization. Annu Rev Physiol. 2017; 79: 541–566, doi: 10.1146/annurev-physiol-022516-034339, indexed in Pubmed: 27813830.
47. Inoue A, Matsumoto I, Tanaka Y, et al. Tumor necrosis factor alpha-induced adipose-related protein expression in experimental arthritis and in rheumatoid arthritis. Arthritis Res Ther. 2009; 11(4): R118, doi: 10.1186/ar2779, indexed in Pubmed: 19660107.
48. Han Lu, Tang MX, Ti Y, et al. Overexpressing STAMP2 improves insulin resistance in diabetic ApoE$^{-/-}$/LDLR$^{-/-}$ mice via macrophage polarization shift in adipose tissues. PLoS One. 2013; 8(11): e78903, doi: 10.1371/journal.pone.0078903, indexed in Pubmed: 24236066.
49. Wheeler AP, Bernard GR. Treating patients with severe sepsis. N Engl J Med. 1999; 340(3): 207–214, doi: 10.1056/NEJM199901213400307, indexed in Pubmed: 9895401.
50. Li K, He Z, Wang X, et al. Apigenin C-glycosides of Microcos paniculata protects lipopolysaccharide induced apoptosis and inflammation in acute lung injury through TLR4 signaling pathway. Free Radic Biol Med. 2018; 124: 163–175, doi: 10.1016/j.freeradbiomed.2018.06.009, indexed in Pubmed: 29890216.
51. Hotchkiss RS, Nicholson DW. Apoptosis and caspases regulate death and inflammation in sepsis. Nat Rev Immunol. 2006; 6(11): 813–822, doi: 10.1038/nri1943, indexed in Pubmed: 17039247.
52. Moon SJ, Kim HY, Kim YH, et al. GADD45β plays a protective role in acute lung injury by regulating apoptosis in experimental sepsis in vivo. J Cell Physiol. 2018; 233(10): 7128–7138, doi: 10.1002/jcp.26635, indexed in Pubmed: 29741778.
53. Swanton E, Savory P, Cosulich S, et al. Bcl-2 regulates a caspase-3/caspase-2 apoptotic cascade in cytosolic extracts. Oncogene. 1999; 18(10): 1781–1787, doi: 10.1038/sj.onc.1202490, indexed in Pubmed: 10086332.
54. Wang J, Han Lu, Wang Zh, et al. Overexpression of STAMP2 suppresses atherosclerosis and stabilizes plaques in diabetic mice. J Cell Mol Med. 2014; 18(4): 735–748, doi: 10.1111/jcmm.12222, indexed in Pubmed: 24467451.
55. Zheng H, Liang W, He W, et al. Ghrelin attenuates sepsis-induced acute lung injury by inhibiting the NF-κB, iNOS, and Akt signaling in alveolar macrophages. Am J Physiol Lung Cell Mol Physiol. 2019; 317(3): L381–L391, doi: 10.1152/ajplung.00253.2018, indexed in Pubmed: 31242025.
56. Yu YY, Li XQ, Hu WP, et al. Self-developed NF-κB inhibitor 270 protects against LPS-induced acute kidney injury and lung injury through improving inflammation. Biomed Pharmacother. 2022; 147: 112615, doi: 10.1016/j.biopha.2022.112615, indexed in Pubmed: 35026488.
57. Jiao Y, Zhang Ti, Zhang C, et al. Exosomal miR-30d-5p of neutrophils induces M1 macrophage polarization and primes macrophage pyroptosis in sepsis-related acute lung injury. Crit Care. 2021; 25(1): 356, doi: 10.1186/s13054-021-03775-3, indexed in Pubmed: 34641966.
58. ten Freyhaus H, Calay ES, Yalcin A, et al. Stamp2 controls macrophage inflammation through nicotinamide adenine dinucleotide phosphate homeostasis and protects against atherosclerosis. Cell Metab. 2012; 16(1): 81–89, doi: 10.1016/j.cmet.2012.05.009, indexed in Pubmed: 22704678.
59. Wang N, Liang H, Zen Ke. Molecular mechanisms that influence the macrophage m1-m2 polarization balance. Front Immunol. 2014; 5: 614, doi: 10.3389/fimmu.2014.00614, indexed in Pubmed: 25506346.
60. Zhang J, Wang C, Wang H, et al. Loganin alleviates sepsis-induced acute lung injury by regulating macrophage polarization and inhibiting NLRP3 inflammasome activation. Int Immunopharmacol. 2021; 95: 107529, doi: 10.1016/j.intimp.2021.107529, indexed in Pubmed: 33744777.
61. Mollenhauer M, Bokredenghel S, Geißen S, et al. Stamp2 protects from maladaptive structural remodeling and systolic dysfunction in post-ischemic hearts by attenuating neutrophil activation. Front Immunol. 2021; 12: 701721, doi: 10.3389/fimmu.2021.701721, indexed in Pubmed: 34691017.

Submitted: 3 August, 2022
Accepted after reviews: 12 December, 2022
Available as AoP: 30 December, 2022